

EXPERIMENTAL DEVELOPMENT AND MOLECULAR DOCKING: NANOSTRUCTURED LIPID CARRIERS (NLCs) OF COENZYME Q10 USING STEARIC ACID AND DIFFERENT LIQUID LIPIDS AS LIPID MATRIX

NI LUH DEWI ARYANI^{1,3}, SISWANDONO², WIDJI SOERATRI^{1*}, FANNY PUTRI RAHMASARI³, DIAN RIZKI KARTIKA SARI³

¹Department of Pharmaceutics, Faculty of Pharmacy, Airlangga University, Surabaya, Indonesia, ²Department of Pharmaceutical Chemistry, Faculty of Pharmacy, Airlangga University, Surabaya, Indonesia, ³Department of Pharmaceutics, Faculty of Pharmacy, University of Surabaya, Surabaya, Indonesia
Email: widji-s@ff.unair.ac.id

Received: 30 Sep 2020, Revised and Accepted: 20 Nov 2020

ABSTRACT

Objective: To develop coenzyme Q10 (co-Q10) nanostructured lipid carriers (NLCs) using stearic acid (SA) and various liquid lipids with different lipophilicity as well as highlights the use of *in silico* studies for predicting and elucidating the interaction of drug-lipid used as carries in NLCs, at the molecular level.

Methods: The co-Q10 NLCs were prepared using SA as solid lipid and oleic acid (OA), isopropyl myristate (IPM), as well as isopropyl palmitate (IPP) as liquid lipids by the high shear homogenization method. Firstly, the formulas were optimized by the appropriate required HLB (rHLB). The optimized NLCs were characterized in the particle size, distribution of particle size, zeta potential, crystallinity behavior, Fourier transform infrared (FT-IR) spectra, morphology, entrapment efficiency (EE), drug loading (DL), and pH value. The interaction of drug-lipids *in silico* was studied using the AutoDock Vina program.

Results: The co-Q10 NLCs using SA and the various liquid lipid possessed the mean particle size, polydispersity index (PDI), zeta potential, EE, DL, and pH values were 180 to 350 nm, <0.5, <-30 mV, 83 to 88%, 10 to 11%, and 5.0 to 5.6, respectively. The EE and DL of co-Q10 NLCs increased with decreasing in binding energy (ΔG) *in silico*.

Conclusion: The co-Q10 NLCs using SA as solid lipid and OA, IPM, as well as IPP as liquid lipids were developed successfully. Furthermore, *in silico* study by molecular docking is a potential approach in predicting and elucidating the interaction of drug-lipid in the development of NLCs formulation.

Keywords: Coenzyme Q10, Nanostructured lipid carriers, Stearic acid, Molecular docking

© 2021 The Authors. Published by Innovare Academic Sciences Pvt Ltd. This is an open access article under the CC BY license (<http://creativecommons.org/licenses/by/4.0/>)
DOI: <http://dx.doi.org/10.22159/ijap.2021v13i1.39890>. Journal homepage: <https://innovareacademics.in/journals/index.php/ijap>

INTRODUCTION

Co-Q10 is an antioxidant that can be used as a skin anti-aging. Co-Q10 is lipophilic because it has 10 isoprene side chains. The chemical structure of co-Q10 is shown in fig. 1. Due to its lipophilic properties, the penetration of co-Q10 through the skin is low [1, 2]. This problem can be overcome using NLC.

NLC is the second generation of the lipid nanoparticle delivery system. NLCs have lipid carriers consisting of a mixture of solid lipids and liquid lipids [3, 4]. The main components of NLC are lipids, surfactants, and water [5]. These components determine emulsion stability during the NLC production process. The required hydrophilic-lipophilic balance (rHLB) value of the lipid matrix should be matched to the HLB value of the surfactants to obtain stable emulsion [6, 7].

Co-Q10

SA

OA

IPM

IPP

Fig. 1: Chemical structure of co-Q10, SA, OA, IPM, IPP

In the present study, Tween 80 (HLB=15) and Span 80 (HLB=4.3) [8] were used as a combination of surfactants, SA as a solid lipid, OA, IPM, and IPP as liquid lipids. The liquid lipids have different lipophilicity. The chemical structure of SA, OA, IPM, and IPP is shown in fig. 1. The co-Q10 NLCs were characterized in particle size, PDI, zeta potential, morphological, differential scanning calorimetry (DSC) thermogram, FT-IR spectra, EE, DL, and pH values. Evaluation *in silico* was also performed by molecular docking to predict and elucidate the interaction between co-Q10 and the liquid lipids used. The interaction between co-Q10 and liquid lipids was analyzed through ΔG . Low ΔG shows stable interactions between molecules [9] and it can affect EE and DL [10].

MATERIALS AND METHODS

Materials

Co-Q10 was purchased from Kangcare Bioindustry Co., Ltd. (Nanjing, China). SA, IPP, IPM, propylene glycol, Tween 80 were purchased from Bratachem (Surabaya, Indonesia). OA, Span 80, phenoxyethanol were purchased from Universal Pharma Chemical (Surabaya, Indonesia). Sodium dihydrogen phosphate p. a., disodium

hydrogen phosphate p. a., ethanol 96% p. a. were purchased from E. Merck (Darmstadt, Germany). All materials used in the study have a pharmaceutical-grade unless otherwise stated.

Methods

Molecular docking

The chemical structure and International Union of Pure and Applied Chemistry (IUPAC) name of co-Q10, OA, IPM, and IPP were confirmed using PubChem®. The three dimensional (3D) chemical structure of co-Q10 and liquid lipids were obtained using ChemOffice Pro 2016, and the energy minimization process was carried out using the same program. The files were saved in the cdx file format. Files with the cdx format were converted to file. pdb using the Discovery Studio Visualizer (DSV). File. pdb from DSV becomes file. pdbqt on AutoDock Tools (ADT). Molecular docking of co-Q10 and various lipids were run using AutoDock Tools 1.5.6 and AutoDock Vina. Spacing (Armstrong) was selected 1, the position and size of the grid box were arranged so that all the structure of co-Q10 and liquid lipids were in the grid box, as shown in table 1. The number of molecular docking processes was 10 times. Visualization of docking results used DSV and ADT.

Table 1: Position and size of the grid box in the molecular docking process

Molecule	Grid box		
	Parameter	Center	Size
Co-Q10 and OA	X	-1.54	126
	Y	-2.404	126
	Z	-0.489	124
Co-Q10 and IPM	X	-1.54	126
	Y	-2.404	104
	Z	-0.489	110
Co-Q10 and IPP	X	-1.54	98
	Y	-2.404	126
	Z	-0.489	106

Formulation of co-Q10 NLCs

SA was put into liquid lipids then it was melted at 80 °C and stirred until homogeneous for about 1 min at 3400 rpm with ultra turrax. Co-Q10 was added to the lipid mixture and stirred until it dissolved for about 2 min. Separately, Span 80 and tween 80 were heated to 80 °C, added sequentially, and stirred until homogeneous for about 1 min. The phosphate buffer and propylene glycol were heated to 80 °C separately from the lipid phase. The mixture was added slowly to the lipid phase and stirred until it was homogeneous for about 1 min. After that, the mixture was stirred at 24 000 rpm for 3 min. After 3 min the stirring speed was changed to 3400 rpm.

Phenoxyethanol was added to the mixture at 40 °C and stirred continuously until room temperature.

Optimization of co-Q10 NLCs formula

Several formulas with different rHLB and different concentrations of the lipid matrix were evaluated to obtain physically stable NLCs. The physical stability of the NLCs was evaluated for 10 d at room temperature by visual examination. The stable NLCs did not show phase separation or breaking. The formulations to determine the rHLB and the concentrations of the lipid matrix of the co-Q10 NLCs were presented in table 2.

Table 2: The Formulations for rHLB determination of the co-Q10 NLC (concentration of materials given in %)

Material	Surfactant (10%)				Surfactant (20%)			
	Lipid (8%)		Lipid (10%)		Lipid (8%)			
	rHLB 13	rHLB 14	rHLB 14	rHLB 13	rHLB 14			
Co-Q10	F1	F2	F3	F4	F5	F6	F7	F8
Co-Q10	1.0	1.0	1.0	1.0	1.0	1.0	1.0	1.0
SA	5.6	5.6	5.6	7	7	5.6	5.6	5.6
OA	-	-	-	-	-	2.4	-	-
IPM	2.4	-	-	-	-	-	2.4	-
IPP	-	2.4	2.4	3	3	2.4	2.4	2.4
Tween 80	8.1	8.1	9.0	9.0	16.2	18	18	18
Span 80	1.9	1.9	1.0	1.0	3.8	2	2	2
Propylene glycol	10.0	10.0	10.0	10.0	10.0	10.0	10.0	10.0
Phenoxyethanol	0.6	0.6	0.6	0.6	0.6	0.6	0.6	0.6
Phosphate buffer pH 5.5 up to	100	100	100	100	100	100	100	100

Physicochemical characterization of the co-Q10 NLCs

Particle size, polydispersity index, and zeta potential

The particle size, polydispersity index, and zeta potential were measured by the dynamic light scattering (DLS) method using the nanoparticle analyzer (Nanotracs Wave, Microtracs W3717).

Morphology of the co-Q10 NLCs

The morphology of the co-Q10 NLCs was performed using scanning electron microscopy (SEM, ZEISS). The samples were applied to an object-glass and dried at 40-50 °C using a hot plate. After that, the samples were coated with gold and observed by SEM with magnifications of 10 000x and 25 000x.

Differential scanning calorimetry (DSC)

DSC was used to determine the melting temperature and crystallinity of co-Q10, SA, and co-Q10 NLCs. The weighted sample (4 mg) was put into an aluminum pan and heated from 30 to 100 °C in a calorimeter (DSC model 1/500, Mettler Toledo). The heating rate of the calorimeter was 10 °C/min. The percentage of crystallinity index (CI) is measured by the following equation [6]:

$$CI (\%) = \frac{\Delta H \text{ NLC coenzyme Q10}}{\Delta H \text{ lipid matrix} \times \text{concentration lipid phase}} \times 100 \text{----(1)}$$

Where ΔH co-Q10 NLC and ΔH lipid matrix are the melting enthalpy (J/g) of the co-Q10 NLC and solid lipid (SA), respectively.

Fourier transform infrared (FT-IR)

FT-IR spectra of the samples were obtained using an FT-IR spectrophotometer (Jasco FT-IR 5300). The samples were added to KBr powder and compressed with a hydraulic press to obtain a transparent plate. The plate was scanned at wavelengths of 400-4000 cm^{-1} .

Entrapment efficiency (EE) and drug loading (DL)

The EE of co-Q10 NLC was obtained by indirect methods. The untrapped Co-Q10 in NLC was obtained through the centrifugation method. The co-Q10 NLC was diluted with aqua dem quantitatively and put into Amicon® Ultra-15 tubes with 30 kDa molecular weight cut-offs (Merck Millipore) then centrifuged at 10 000 rpm for 30 min. The absorbance of the filtrate was measured using a UV spectrophotometer at a wavelength of 275 nm [11].

EE is calculated using the following equation:

$$EE (\%) = \frac{(Ca - Cb)}{Ca} \times 100 \text{----(2)}$$

DL is calculated using the following equation

$$DL (\%) = \frac{Da - Db}{DL} \times 100 \text{----(3)}$$

Where Ca is the initial concentration of co-Q10 in NLC, Cb is the concentration of free co-Q10 in the filtrate, Da is the initial amount of co-Q10 in NLC, Db is the amount of free co-Q10 in the filtrate, DL is the amount of lipid in co-Q10 NLC.

The pH value

The pH values of the co-Q10 NLCs were evaluated using a calibrated pH meter.

Data analysis

Differences in the particle size, EE, DL, and pH value of the co-Q10 NLCs were analyzed using one-way ANOVA statistical methods,

which were followed by Tuckey Honestly test to see different data pairs. The results were considered to be a statistically significant difference at p -value < 0.05. The correlation between *in silico* and *in vitro* study was analyzed by regression analysis. There is a significant relationship if the correlation coefficient (r) > 0.9877.

RESULTS AND DISCUSSION

Molecular docking

The results of molecular docking between co-Q10 and liquid lipids showed that ΔG *in silico* of co-Q10-IPP was the lowest. This shows that IPP had the highest affinity for co-Q10. IPP has the longest hydrocarbon chain so that the lipophilicity is highest [12]. Due to the highest lipophilicity leads to the affinity of IPP to co-Q10 is highest. The ΔG *in silico* of co-Q10-OA, co-Q10-IPM, and co-Q10-IPP were -4.9, -5.7, and -6.5 kcal/mol, respectively, as presented in table 5.2. A negative ΔG value indicates that the interaction between fatty acid molecules and the co-Q10 can occur spontaneously [13, 14].

The 3D visualization of molecular docking using DSV showed that there were the hydrophobic bonds in co-Q10-OA, co-Q10-IPM, and co-Q10-IPP, as shown in fig. 2. The C18 atom of OA forms hydrophobic bonds with the C58 and C59 atoms of co-Q10 with a distance of 3.72 and 4.09 Å, respectively. The C14 atom and C15 atom of IPM form hydrophobic bonds with the C56 atom and the C51 atom of co-Q10 with a distance of 4.01 Å and 4.48 Å, respectively. The C18 atom of IPP forms a hydrophobic bond with the C51 atom of co-Q10 with a distance of 3.96 Å. The results of molecular docking in the previous study also showed the hydrophobic bond in co-Q10-docosahexaenoic acid (DHA) and co-Q10-eicosapentaenoic acid (EPA). Docosahexaenoic acid and eicosapentaenoic acid are chemical content of fish oil, which was used as a carrier of the oleogel formulation [15].

Intermolecular interactions can be in the form of ionic, ion-dipole, and dipole-dipole bonds, hydrogen bonds, van der Waals bonds, and hydrophobic bonds [9]. The 3D visualization of co-Q10-OA, co-Q10-IPM, and co-Q10-IPP using the DSV only show hydrophobic interactions. The van der Waals interaction could not be shown in the interaction of these molecules because of the limitations of the software used. The van der Waals interactions can occur in non-polar molecules [14]. It is attractive forces between molecules or atoms that are not charged and are located close to a distance of ± 4 -6 Å. The van der Waals interaction occurs due to the polarity of the induced atoms. It is a weak interaction, but if a large amount can produce significant ΔG in the interactions between molecules [9]. Co-Q10, OA, IPM, and IPP are non-polar [12]. These molecules showed van der Waals interactions using ADT, as shown in fig. 3.

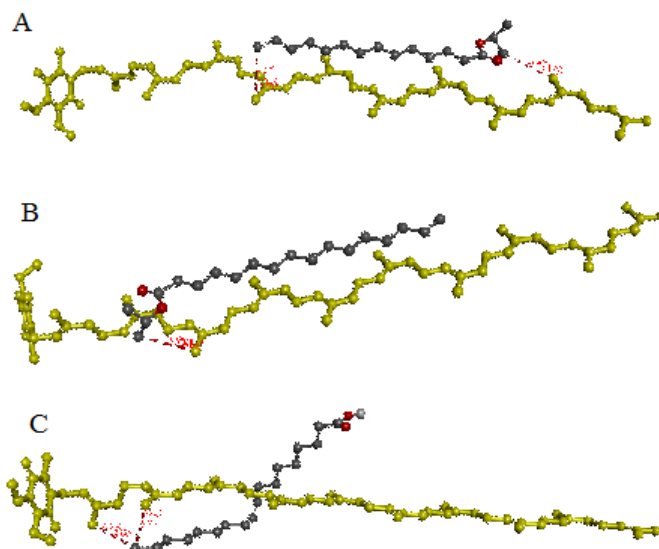


Fig. 2: Docking of co-Q10 with OA (A), IPM (B), and IPP (C) using DSV show hydrophobic bonds

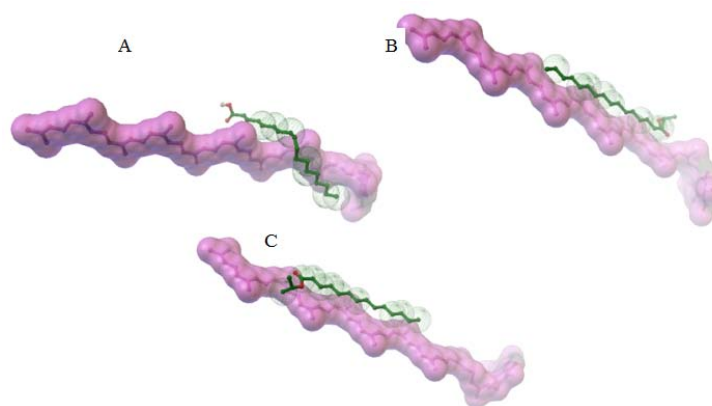
Table 3: The binding energies of co-Q10 with various liquid lipids by molecular docking

Liquid lipids	IUPAC name	ΔG (kcal/mol)
OA (C ₁₈ H ₃₄ O ₂)	(~{Z})-octadec-9-enoic acid	-4.9
IPM (C ₁₇ H ₃₄ O ₂)	Propan-2-yl tetradecanoate	-5.7
IPP (C ₁₉ H ₃₈ O ₂)	Propan-2-yl hexadecanoate	-6.5

Optimization of co-Q10 NLCs formula

The main components of NLC are solid lipids, liquid lipids, surfactants, and water [16]. These components are the factors that

determine the formation of a stable emulsion during the NLC manufacturing process. The required HLB (rHLB) of matrix lipid and amount of surfactants are the factors that determining emulsion stability [6, 7, 17-19].

**Fig. 3 Docking co-Q10 with OA (A), IPM (B), and IPP (C) using ADT show van der Waals interactions**

In this study, the surfactants were a combination of Tween 80 and span 80. The optimization of the formula used 10 and 20% surfactants, with rHLB values of 13 and 14. The lipid matrix concentrations were 8 and 10%. The stability of the co-Q10 NLCs was evaluated for 10 d at room temperature to select the optimal formula.

The results of the stability test visually of co-Q10 NLC at room temperature for 10 d are shown in table 4. The co-Q10 NLC (F6), (F7), and (F8) were not breaking. The co-Q10 NLC (F6), (F7), and (F8) used an 8% lipid matrix with rHLB value 14, 20% surfactants as well as OA, IPM, and IPP as liquid lipids, respectively. Then the optimized NLCs were characterized physicochemically.

Table 4: The physical stability by visual evaluation

Formula	Physical stability
Co-Q10 NLC (F1)	Breaking
Co-Q10 NLC (F2)	Breaking after 7 d
Co-Q10 NLC (F3)	Breaking after 10 d
Co-Q10 NLC (F4)	Breaking after 4 d
Co-Q10 NLC (F5)	Breaking after 10 d
Co-Q10 NLC (F6)	Not breaking
Co-Q10 NLC (F7)	Not breaking
Co-Q10 NLC (F8)	Not breaking

Physicochemical characterization of the co-Q10 NLCs**Particle size, polydispersity index, and zeta potential**

The particle size of the co-Q10 NLCs (F6) was largest, while the particle sizes of the co-Q10 NLCs (F7) and (F8) were not different, as shown in table 5. The particle size of transdermal delivery systems is smaller than 600 nm and the particle size of drug < 300 nm is optimal for penetration through the skin [20].

The PDI of co-Q10 NLCs (F6), (F7), and (F8) were < 0.5, as shown in table 5. This indicates that the particle size distribution of the co-Q10 NLCs (F6), (F7), and (F8) were homogenous [21, 22].

The zeta potential of co-Q10 NLCs (F6), (F7), and (F8) were < -30 mV, as shown in table 5, that indicated the formulas have good stability. The negative zeta potential values of co-Q10 NLC (F6), (F7), and (F8) were caused by the carboxyl group of SA. The negative zeta potential of the nano lipid particle delivery system using SA as a lipid matrix was also obtained in the earlier studies [23-25].

Table 5: Particle size, PDI, and zeta potential of co-Q10 NLCs

Formula	Parameter		
	Particle size (nm)	PDI	Zeta potential (mV)
Co-Q10 NLC (F6)	356.0±28.8	0.3100±0.1000	-41.4±5.6
Co-Q10 NLC (F7)	236.4±48.8	0.3167±0.0900	-46.8±12.3
Co-Q10 NLC (F8)	184.2±16.3	0.1838±0.1110	-54.6±1.0

mean±SD (n=3)

Morphology of the co-Q10 NLCs

To obtain information about the morphology of the co-Q10 NLCs, SEM analysis was performed. The micrograph of the co-Q10 NLCs

(F6), (F7), and (F8) illustrated spherical particles and relatively smooth surface as shown in fig. 4, 5, and 6. The sticky nature of the lipid and sample preparation process for SEM analysis were probably the causes of the presence of some aggregates [26].

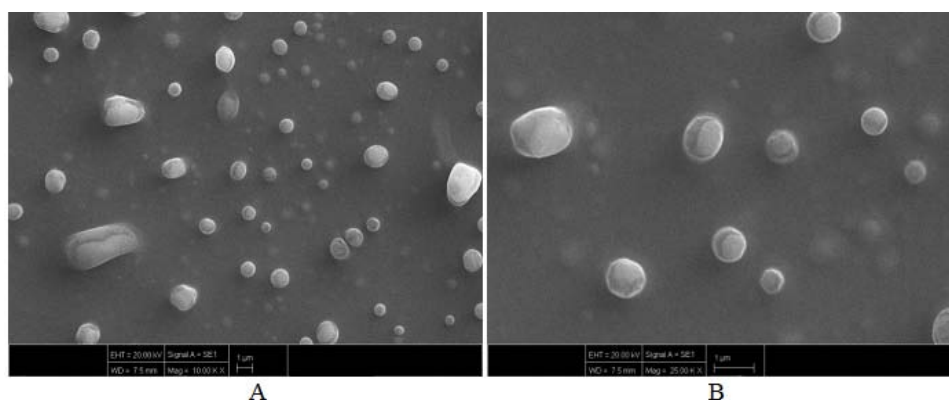


Fig. 4: SEM image of co-Q10 NLC (F6) with magnification of (A) 10 000x and (B) 25 000x

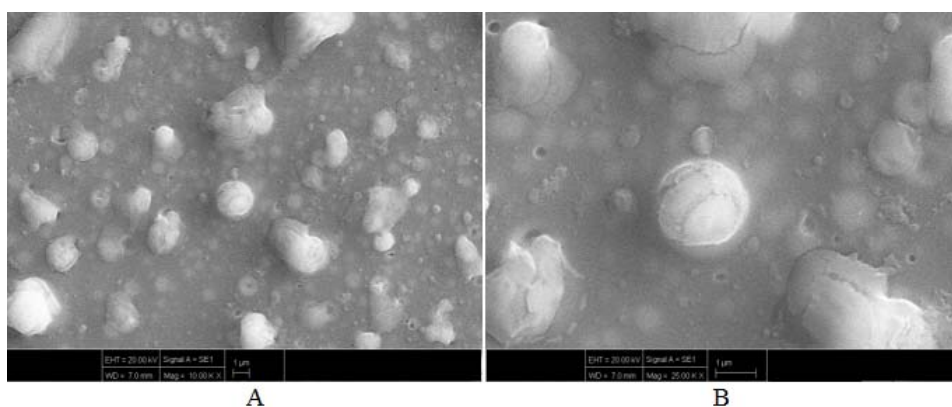


Fig. 5: SEM image of co-Q10 NLC (F7) with magnification of (A) 10 000x and (B) 25 000x

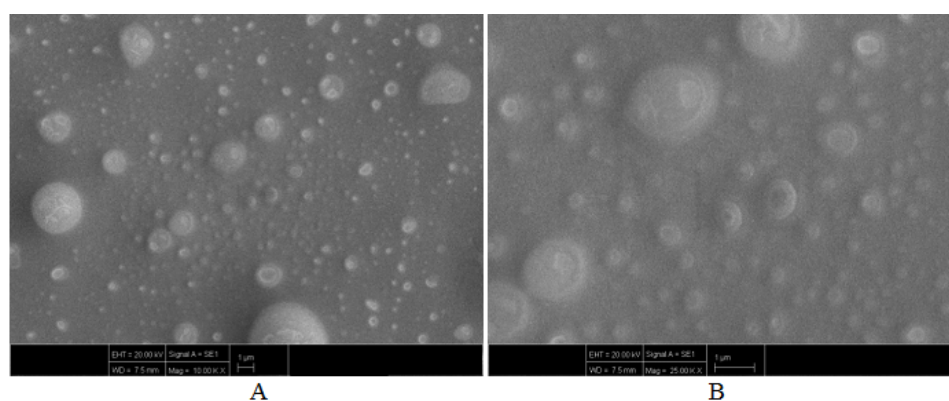


Fig. 6: SEM image of co-Q10 NLC (F8) with magnification of (A) 10 000x and (B) 25 000x

Table 6: Melting point, melting enthalpy (ΔH), and (CI)

Material	Melting point (°C)	ΔH (J/g)	CI (%)
Co-Q10	51.63	-153.2	-
SA	58.01	-190.12	100
Co-Q10 NLC (F6)	46.44	-4.32	28.40
Co-Q10 NLC (F7)	45.30	-5.47	35.96
Co-Q10 NLC (F8)	45.16	-5.01	32.94

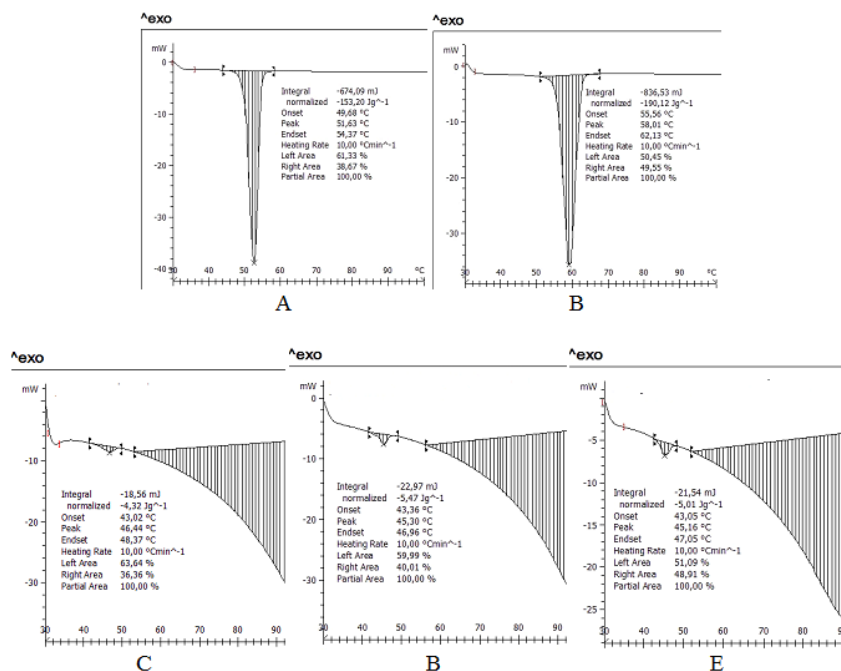


Fig. 7: DSC thermogram of co-Q10 (A), SA (B), co-Q10 NLC (F6) (C), co-Q10 NLC (F7) (D), and co-Q10 NLC (F8) (E)

Differential scanning calorimetry (DSC)

The crystalline or amorphous nature of the co-Q10 NLCs (F6), (F7), and (F8) were analyzed by DSC. The DSC thermograms, melting point, and enthalpy of coenzyme Q10, SA, co-Q10 NLC (F6), co-Q10 NLC (F7), and co-Q10 NLC (F8) are presented in fig. 7 and table 6.

The melting points of co-Q10, SA, co-Q10 NLC (F6), (7), and (8) showed endothermic peaks at 51.63, 58.01, 46.44, 45.30, and 45.16 °C, respectively.

The melting enthalpies of co-Q10, SA, co-Q10 NLCs (F6), (F7), and (F8) were -153.2, -190.12, -4.32, -5.47, and -5.01 J/g, respectively. The melting point and melting enthalpy of co-Q10 NLC (F6), (F7), and (F8) were decreased compared with the melting point and the melting enthalpy of co-Q10 and SA. It is due to co-Q10 that was presented in the amorphous phase and dispersed homogeneously into the lipid matrix.

The CI was calculated by comparing the enthalpy of co-Q10 NLC with the enthalpy of SA (equation 1). Lipid crystallinity affects EE and DL [7, 27]. The CI of co-Q10 NLC (F6), (F7), and (F8) are presented in table 6. The CI of SA was 100%. The addition of liquid lipids in the formula causes the enthalpy of co-Q10 NLC (F6), (F7), and (F8) was decreased compared with the enthalpy of SA. So, the CI of co-Q10 NLC (F6), (F7), and (F8) were smaller than the CI of SA. A

similar result was also obtained from an earlier study, that the CI of NLC was decreased compared with the CI of the lipid used (carnauba wax, Compritol 888 AT0, and beeswax with certain liquid lipids) [28]. This is due to liquid lipids decreases the orderedness of the solid lipid crystal structures [4].

Fourier transform infrared (FT-IR)

The FT-IR spectra of co-Q10, co-Q10 NLCs, and the lipids in the region of 4000–400 cm⁻¹ is shown in fig. 8 to fig 10. The FT-IR spectra of co-Q10 exhibit peaks at 2962.13, 1732.73, 1645.95, and 1200.47 cm⁻¹ for C-H stretching, C=O stretching, C=C stretching and C-O stretching, respectively. The FT-IR spectra of co-Q10 NLCs did not present new peaks if compared with the FT-IR spectra of co-Q10, and the lipids. It was due to there were no chemical interactions that lead to forming new functional groups in the co-Q10 NLC. Co-Q10 is only entrapped in the lipid matrix [29, 30]. This was also proved by DSC thermograms that indicated co-Q10 was entrapped in the lipid matrix. Due to nonpolar molecules, the possible interactions between co-Q10 and matrix lipids are hydrophobic and van der Waals [14]. The molecular docking studies of co-Q10 and the lipids used showed hydrophobic and van der Waals interactions. The hydrophobic and van der Waals interactions did not lead to forming new functional groups.

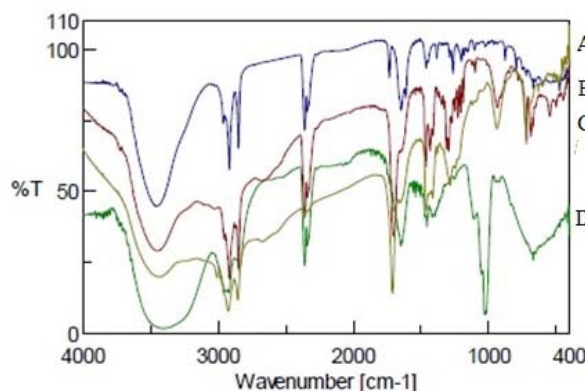


Fig. 8: FT-IR Spectra of co-Q10 (A), OA (B), SA (C), and co-Q10 NLC (F6) (D)

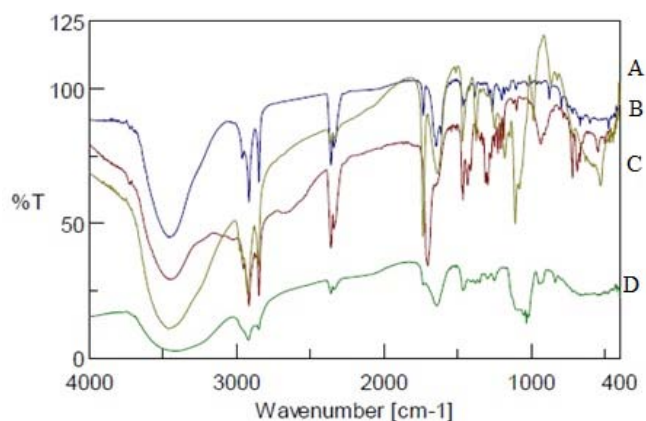


Fig. 9: FT-IR spectra of co-Q10 (A), IPM (B), SA (C), and co-Q10 NLC (F7) (D)

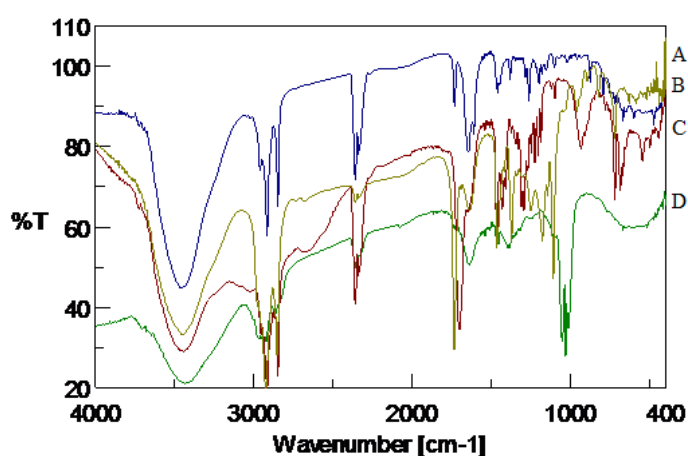


Fig. 10: FT-IR spectra of co-Q10 (A), IPP (B), SA (C), and co-Q10 NLC (F8) (D)

Entrapment efficiency (EE) and drug loading (DL)

The EE of the co-Q10 NLC (F6, (7) and (F8) were >80%, as shown in table 7. These were due to the addition of liquid lipids into the

SA lead to order crystal structure became disordered. Disorders of the crystal structure leave enough space for the incorporation of drug molecules [27]. The EE and DL of co-Q10 NLC (F8) were the highest.

Table 7: EE and DL of co-Q10 NLCs

Formula	EE (%)	DL (%)
Co-Q10 NLC (F6)	82.840±0.791	10.355±0.099
Co-Q10 NLC (F7)	84.225±2.119	10.528±0.265
Co-Q10 NLC (F8)	87.799±2.181	10.975±0.273

mean±SD (n=3)

Table 8: The pH values of co-Q10 NLC (F6), (F7), and (F8)

Formula	pH
Co-Q10 NLC (F6)	5.55±0.01
Co-Q10 NLC (F7)	5.67±0.04
Co-Q10 NLC (F8)	5.50±0.07

mean±SD (n=3)

The co-Q10 NLCs pH value

The co-Q10 NLC (F6), (F7), and (F8) possessed pH values similar to the pH value of the skin. The skin pH value is 4-6.5 [31]. The pH values of co-Q10 NLC (F6), (F7), and (F8) were about 5. The pH values co-Q10 NLC (F6), (F7), and (F8) are presented in table 8.

The correlation of the EE or DL *in vitro* and the ΔG *in silico*

Besides the crystallinity of lipids, the EE and DL in NLC also depend on the nature of the drug and lipids. The nature of the drug and lipids affect the interaction between them. Co-Q10 is a lipophilic substance (log P=21) [1], so it has good interaction with lipids.

To evaluate the influencing of interactions drug-lipid on EE and DL, the regression analysis between EE or DL and ΔG *in silico* was

performed. The correlation curve between EE or DL and the ΔG *in silico* is presented in fig. 11.

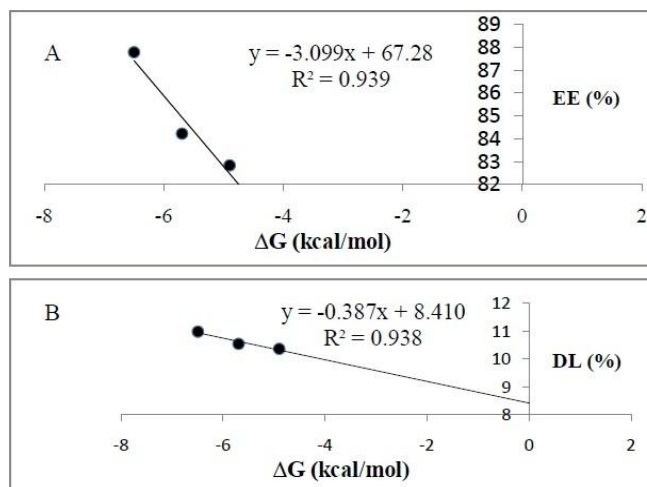


Fig. 11: Correlation of ΔG *in silico* and EE (A) and DL (B) of co-Q10 NLCs

Although the non-fitting correlations were observed between EE or DL of co-Q10 NLCs *in vitro* and ΔG *in silico*, the EE and DL of co-Q10 NLCs increased with decreasing in ΔG *in silico*. Similar results were also obtained from a previous study, that studied the interactions between amorphous chitin nanoparticles with three different types of anti-cancer drugs such as curcumin, docetaxel, and 5-fluorouracil by the integration of *in silico* and *in vitro* studies [32].

CONCLUSION

The development of co-Q10 NLCs using SA as solid lipid and OA, IPM, and IPP as liquid lipids were prepared successfully using the appropriate rHLB. The NLCs possessed the mean particle size, PDI, zeta potential were about 180-350 nm, <0.5, <-0.3 mV, respectively. The NLCs particles were spherical. The pH values of the co-Q10 NLCs met the skin pH. Co-Q10 was entrapped and dissolved in the lipid matrix, it was indicated from the FT-IR spectra and supported by *in silico* studies. The molecular docking exhibited hydrophobic bonds and van der Waals interaction between molecule co-Q10 and the lipids. The DSC studies showed that the crystallinity index of co-Q10 NLCs was smaller than SA, so it influenced the EE and DL of the co-Q10 NLCs. The EE of the co-Q10 NLCs 83 to 88% and DL 10 to 11%. The EE and DL of the co-Q10 NLCs increased with a decrease in ΔG *in silico*. So *in silico* study is a potential approach in predicting and elucidating the interaction of drug-lipid in the development of NLCs.

FUNDING

This research was funded by Surabaya University.

AUTHORS CONTRIBUTIONS

All the authors have contributed equally.

CONFLICT OF INTERESTS

The authors declare no conflict of interest among themselves.

REFERENCES

- Zaki NM. Strategies for oral delivery and mitochondrial targeting of CoQ10. *Drug Delivery* 2016;23:1868-81.
- Korkmaz E, Gokce EH, Ozer O. Development and evaluation of coenzyme Q10 loaded solid lipid nanoparticle hydrogel for enhanced dermal delivery. *Acta Pharm* 2013;63:517-29.
- Müller RH, Staufenbergel S, Keck C. Lipid nanoparticles (SLN, NLC) for innovative consumer care and household products. *Househ Pers Care Today* 2014;9:18-25.
- Naseri N, Valizadeh H, Zakeri Milani P. Solid lipid nanoparticles and Nanostructured lipid carriers: Structure preparation and application. *Adv Pharm Bull* 2015;5:305-13.

- Fang CL, Al-Suwayeh S, Fang JY. Nanostructured lipid carriers (NLCs) for drug delivery and targeting. *Recent Pat Nanotechnol* 2012;7:41-55.
- Keck CM, Baisaeng N, Durand P, Prost M, Meinke MC, Müller RH. Oil-enriched, ultra-small Nanostructured lipid carriers (usNLC): a novel delivery system based on flip-flop structure. *Int J Pharm* 2014;477:227-35.
- Flavia D, Conrado M, Thallysson Carvalho B, Daniele M, Luciana N, Salvana C, et al. Polymorphism, crystallinity and hydrophilic-lipophilic balance (HLB) of ceteryl alcohol and cetyl alcohol as raw materials for solid lipid nanoparticles (SLN). *ASP Nanotechnol* 2018;1:52-60.
- Rowe RC, Sheskey PJ, Quinn ME. editors. Handbook of pharmaceutical excipient. London: The Pharmaceutical Press; 2015.
- Siswandono. editor. Kimia Medisinal 2. 2nd ed. Surabaya: Airlangga University Press; 2016.
- Hathout RM, Metwally AA. Towards better modeling of drug-loading in solid lipid nanoparticles: molecular dynamics, docking experiments and gaussian processes machine learning. *Eur J Pharm Biopharm* 2016;108:262-8.
- Xia Q, Wang H. Preparation and characterization of coenzyme Q10-loaded nanostructured lipid carries as delivery systems for cosmetic component. *NSTI-Nanotech* 2010;3:498-501.
- Patrick G. Organic chemistry. 2nd ed. Vol. 53. London and New York: Bios Scientific Publishers; 2005.
- Sopyan I, Fudholi A, Muchtaridi M, Sari IP. Co-crystallization: a tool to enhance solubility and dissolution rate of simvastatin. *J Young Pharm* 2017;9:183-6.
- Sinko PJ. editor. Martin's physical pharmacy and pharmaceutical sciences: physical chemical and biopharmaceutical principles in the pharmaceutical sciences: 6th ed. Philadelphia: Lippincott Williams and Wilkins; 2011.
- Zulfakar MH, Chan LM, Rehman K, Wai LK, Heard CM. Coenzyme Q10-loaded fish oil-based bigel system: probing the delivery across porcine skin and possible interaction with fish oil fatty acids. *AAPS PharmSciTech* 2018;19:1116-23.
- Tzachev CT, Svilenov HL. Lipid nanoparticles at the current stage and prospects-a review article. *Int J Pharm Sci Rev Res* 2013;18:103-15.
- Shah R, Eldridge D, Palombo E, Harding I. Optimisation and stability assessment of solid lipid nanoparticles using particle size and zeta potential. *J Phys Sci* 2014;25:59-75.
- Severino P, Andreani T, Macedo AS, Fangueiro JF, Santana MHA, Silva AM, et al. Current state-of-art and new trends on lipid nanoparticles (SLN and NLC) for oral drug delivery. *J Drug Delivery* 2012. DOI:10.1155/2012/750891.

19. Akbari J, Saeedi M, Morteza Semnani K, Rostamkalaei SS, Asadi M, Asare Addo K, *et al.* The design of naproxen solid lipid nanoparticles to target skin layers. *Colloids Surf B* 2016;145:626–33.
20. Danaei M, Dehghankhold M, Ataei S, Hasanzadeh Davarani F, Javanmard R, Dokhani A, *et al.* Impact of particle size and polydispersity index on the clinical applications of lipidic nanocarrier systems. *Pharmaceutics* 2018;10:1–17.
21. Pornputtipitak W, Pantakitcharoenkul J, Panpakdee R, Teeranachaideekul V, Sinchaipanid N. Development of γ -oryzanol rich extract from leum pua glutinous rice bran loaded NLCs for topical delivery. *J Oleo Sci* 2018;67:125–33.
22. Fernandes AV, Pydi CR, Verma R, Jose J, Kumar L. Design, preparation and *in vitro* characterizations of fluconazole loaded NLCs. *Brazilian J Pharm Sci* 2020;56:1–14.
23. Mahajan A, Kaur S. Design, formulation, and characterization of stearic acid-based solid lipid nanoparticles of candesartan cilexetil to augment its oral bioavailability. *Asian J Pharm Clin Res* 2018;11:344–50.
24. Hu FQ, Jiang SP, Du YZ, Yuan H, Ye YQ, Zeng S. Preparation and characterization of stearic acid NLCs by solvent diffusion method in an aqueous system. *Colloids Surf B* 2005;45:167–73.
25. Abdelmonem R, El Nabarawi MA, Attia AM, Teaimaa M. Ocular delivery of natamycin solid lipid nanoparticle loaded mucoadhesive gel: formulation, characterization and *in vivo* study. *Int J Appl Pharm* 2020;12:173–80.
26. Keivani Nahr F, Ghanbarzadeh B, Samadi Kafil H, Hamishehkar H, Hoseini M. The colloidal and release properties of cardamom oil encapsulated NLC. *J Dispers Sci Technol* 2019;1–9. <https://doi.org/10.1080/01932691.2019.1658597>
27. Chauhan I, Mohd Y, Madhu V, SinghPratap A. NLCs: a groundbreaking approach for transdermal drug delivery. *J Cardiovasc Thorac Res* 2015;7:113–7.
28. Chen PC, Huang JW, Pang J. An investigation of optimum NLC-sunscreen formulation using taguchi analysis. *J Nanomater* 2013;7–12. <https://doi.org/10.1155/2013/463732>
29. Siafaka P, Okur ME, Ayla S, Er S, Caglar ES, Okur NU. Design and characterization of nanocarriers loaded with levofloxacin for enhanced antimicrobial activity; physicochemical properties, *in vitro* release and oral acute toxicity. *Brazilian J Pharm Sci* 2019;55:1–13.
30. Remya PN, Damodharan N. Formulation, development, and characterisation of nimodipine loaded solid lipid nanoparticles. *Int J Appl Pharm* 2020;12:265–71.
31. Korting MSHC. The pH of the skin surface and its impact on the barrier function. *Ski Pharmacol Physiol* 2006;19:296–302.
32. Geetha P, Sivaram AJ, Jayakumar R, Gopi Mohan C. Integration of *in silico* modeling, prediction by ΔG and experimental approach to study the amorphous chitin nanocarriers for cancer drug delivery. *Carbohydr Polym* 2016;142:240–9.